33rd Annual International Conference of the IEEE EMBS
Boston, Massachusetts USA, August 30 - September 3, 2011

A SU-8-Based Compact Implantable Wireless Pressure Sensor for Intraocular Pressure Sensing Application

Ning Xue *Student Member, IEEE*, Sung Pil Chang, Jeong-Bong Lee *Senior Member, IEEE*

***Abstract*—Telemetric sensing has received a great deal of attention in noncontact human disease detection. To take advantage of this method, this paper presents a SU-8-based compact (1.52 mm × 3.23 mm × 0.2 mm) passive wireless pressure sensor, especially designed to measure the intraocular pressure. The sensor was microfabricated using biocompatible materials such as gold and SU-8 [1] to form the *LC* parallel circuit and the pressure sensitive diaphragm. The surface of the sensor is fully covered by SU-8, which isolates the working circuit from the biological tissue medium. The pressure signal can be detected by an external readout coil with up to 6 mm distance from the implanted sensor. The pressure sensitivity of the sensor was characterized in both air and saline environment. The microfabricated sensor has high sensitivity (>7,000 ppm/mmHg).**

I. Introduction

INTRAOCULAR pressure (IOP) is the fluid pressure inside the eye between the lens and cornea. It normally has an average level of pressure about 15.7 mmHg above atmosphere with the daily cyclic variations of ±5 mmHg. IOP is a vital aspect to evaluate glaucoma patients whose ocular pressure is higher than 21 mmHg. Therefore, accurate and continuous IOP measurement is necessary to monitor glaucoma patients. However, traditional detection method of IOP using external instruments (contact or noncontact tonometry) is unable to provide real time and long-term measurement. In 1967, Collins [2] proposed that telemetric sensing could be adopted to realize an implantable pressure sensor without leading wires. Among two types of telemetric sensing methods, passive sensors are frequently designed by the researchers because of their simple structure, small size, low cost and low power consumption in contrast to active sensors. With the emergence of microfabrication and MEMS technology, this passive wireless sensing idea was implemented by some researchers and groups [3-6]. However, most of these devices used silicon as the sensor material or as the substrate. Previous study showed that silicon is the least biocompatible compared with other common MEMS materials such as SiO_2, SiN, Au, and SU-8 [7]. From our previous study, we found that SU-8-based implant is biocompatible and there was no apparent sign of tissue damage or inflammatory reaction even after 51 weeks of surgical implantation [1].

Manuscript submitted June 20, 2011.

N. Xue is with Department of Electrical Engineering, University of Texas at Dallas, Richardson, TX 75080 USA (phone: 972-883-2893; fax: 972-883-2710; e-mail: nxx083000@utdallas.edu).

S.P. Chang is with Department of Electrical Engineering, Inha University, Korea (spchang@inha.ac.kr)

J.-B. Lee is with Department of Electrical Engineering, University of Texas at Dallas, Richardson, TX 75080 USA (jblee@utdallas.edu)

In this work, we used SU-8, one of the most commonly used MEMS material, as the key material for a passive pressure sensor for intraocular pressure measurement application.

II. Design

The SU-8-based wireless IOP sensor utilizes inductive coupling as telemetric sensing method. The schematic diagram of the wireless IOP sensor and the detection system are given in Fig. 1, where L_p and R_p are the inductance and resistance of the external coil, respectively, L_s, R_s, C_{s1} are the inductance, resistance and parasitic capacitance of the microfabricated IOP sensor, respectively, C_{s2} is the pressure sensitive variable capacitance of the capacitor.

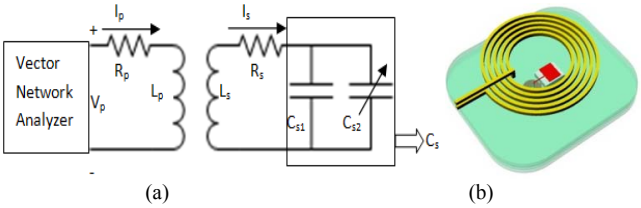

Fig. 1. (a) Equivalent circuit of the IOP sensing system; (b) 3D conceptual schematic diagram of the IOP system. The external coil can be installed at the eyebrow area, whereas the IOP sensor is implanted to the iris of eye.

The relationship of voltage and current can be expressed as

$$\begin{pmatrix} V_p \\ 0 \end{pmatrix} = \begin{pmatrix} R_p + jwL_p & -j\omega M \\ -j\omega M & R_s + jwL_s + \frac{1}{jwC_s} \end{pmatrix} \begin{pmatrix} I_p \\ I_s \end{pmatrix} \quad (1)$$

Then the equivalent impedance can be defined as

$$Z_{eq} = \frac{V_p}{I_p} = R_p + j\omega L_p + \frac{\omega^2 M^2}{R_s + j\omega L_s + \frac{1}{j\omega C_s}} \quad (2)$$

where ω is the working frequency, M is the mutual inductance of the two coils. At the resonant frequency of the IOP sensor (f_{res}), phase dip of the equivalent impedance can be calculated to be

$$\Delta Z_{eq} = 90 - arctan\left(\frac{Im(Z_{eq})}{Re(Z_{eq})}\right) = arctan(Q_s k^2) \quad (3)$$

The phase dip can be enhanced by increasing the Q factor of the IOP sensor (Q_s) and coupling coefficient (k). In our design, electroplated Au was used to decrease the resistance of the IOP sensor, thus increasing Q_s. Thickness of Au was

chosen to be 9 µm, which is two times the skin depth at working frequency (260 MHz).

By considering a fully-clamped circular diaphragm under uniform pressure, maximum deflection d_0 at the center of the plate is

$$d_0 = \frac{Pr^4}{64D}\frac{1}{1+0.488(\frac{d_0}{t_m})^2} \quad (4)$$

where P is the applied pressure, D is the flexural rigidity, r is the radius of diaphragm and t_m is the thickness of diaphragm.

The IOP sensor utilized planar spiral coil as an inductor. The well-known empirical equation to calculate inductance is first given by Wheeler [8] as

$$L(Henry) = 31.33\mu_0 n^2 \frac{a^2}{8a+11c} \quad (5)$$

where μ_0 is the magnetic permeability of free space, n is the number of turns, a is the mean radius of coil in meters, c is the width of winding in meters. Resonant frequency of the IOP sensor was designed to be below 300 MHz, beyond which high power loss occurs in the saline medium. Thus, the designed inductance (L_s) and total capacitance (C_s) of the IOP sensor are 548 µH and 0.72 pF, respectively with its resonant frequency 260 MHz.

The sensitivity of the IOP sensor directly depends on the diaphragm deflection. So thickness of the diaphragm has to be carefully designed in order that maximum deflection can be achieved. However, large deformation can induce nonlinear deflection under linear pressure. Based on the analysis and experimental fabrication limitation, circular diaphragm thickness was chosen to be 18 µm. The deflection of the diaphragm in terms of pressure was theoretically calculated and simulated using COMSOL (Fig. 2). It shows that within the target pressure range (0 - 60 mmHg), the deflection response is relatively linear which is critical for sensor design.

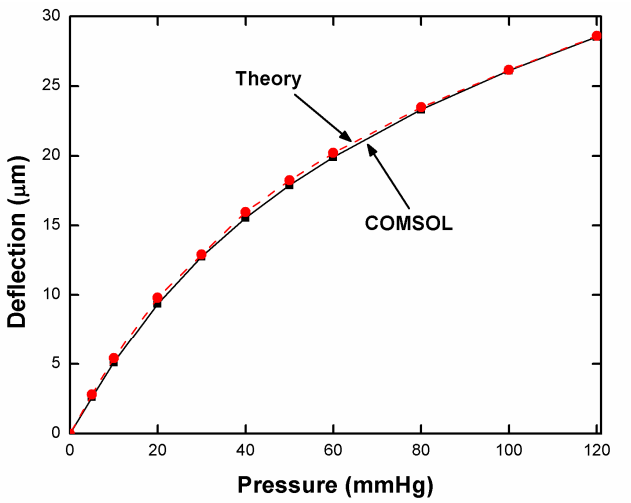

Fig. 2. Deflection of 18 µm thick diaphragm as a function of pressure

III. Fabrication

The IOP sensor consists of SU-8 membrane, a gold inductor and an air gap parallel plate capacitor with SU-8 coated electrodes. The fabrication process is shown in Fig. 3. First of all, 9 µm SU-8 (MicroChem Corp, Newton, MA) was spin coated and patterned on top of an oxidized silicon wafer. A thin Cr/Au seed layer was deposited using sputtering and patterned by positive photoresist SPR-220 (Rohm and Hass, Midland, MI) to expose the coil area. To get high Q factor and subsequently enhance the IOP sensor resolution, 9 µm thick gold was electroplated. Then the seed layer was patterned again to form the bottom plate of the capacitor. Two layers of SU-8 were deposited to create the chamber opening and via hole. Another Cr/Au seed layer was deposited on the purpose of via hole gold electroplating and nickel sacrificial electroplating shown as Fig. 3 (c). Following the previous process, SU-8 layer, Au top plate and SU-8 layer were fabricated accordingly. After accomplishing the main structure of the IOP sensor, nickel was removed using HNO_3/HCl. The whole SU-8-based device structure was then released from the oxidized silicon wafer. Additionally, two layers of SU-8 were fabricated and released from the silicon substrate to serve as the lid of the IOP sensor. A 50 µm thick cavity from the top SU-8 structure was designed to reduce the volume effect of sealed chamber. Finally, the SU-8 lid structure was bonded to the SU-8 function device using biocompatible epoxy glue. Fig. 4 shows the completely released sealed chamber IOP sensor.

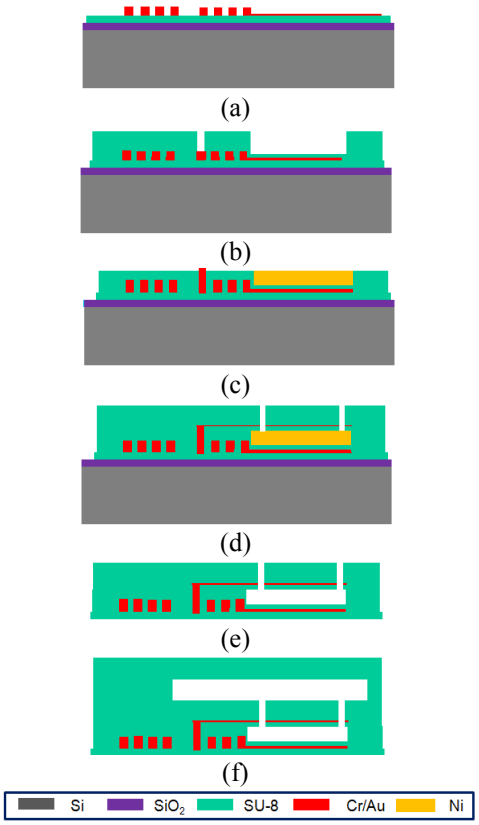

Fig. 3. Wireless IOP sensor fabrication process

(a) (b)

Fig. 4. (a) Optical image of the IOP sensor compared with a US quarter; (b) a photomicrograph of backside view of the IOP sensor

IV. Results and Discussion

A. Electrical parameter measurement

A 25 turns spiral coil with 1.4 mm outer diameter having identical feature with the coil of the IOP sensor was fabricated on Pyrex glass in order to extract the inductance (L_s), resistance (R_s) and parasitic capacitance (C_{s1}) of the coil. Theoretical calculation using Wheeler's equation and HFSS simulation were performed to verify the measurement data. A vector network analyzer (VNA) (Anritsu 37369A) was used to extract electrical parameter of the inductor coil and the *LC* parallel IOP sensor circuit. Table 1 lists the measured electrical data in air and in saline (0.9% NaCl) medium.

TABLE I
ELECTRICAL PARAMETER OF THE WIRELESS IOP SENOR

	Experimental data in air	Experimental data in saline	Simulated data	Theoretical calculated data
Inductance	515 nH	515 nH	560 nH	548 nH
Capacitance	0.95 pF	1.23 pF	--------	0.72 pF
Resonant frequency	228 MHz	200 MHz	--------	260 MHz
Net parasitic capacitance	0.31 pF	0.59 pF	--------	0.205 pF
Q factor	19.4	17	--------	23

The capacitance from the theoretical calculation is 0.23 pF lower than the experimental data in air due to other parasitic capacitances such as SU-8 lid capacitance. Also the resultant experimental capacitance of the IOP sensor in saline solution is higher than the data in the air medium, which can be explained by saline's high dielectric constant, thus increasing the parasitic capacitance. Therefore, the resonant frequency of the device in the saline medium decreases accordingly. Due to the electrical power absorption inside the saline medium, the *Q* factor would decrease inevitably.

B. Pressure testing

The pressure testing setup is shown in Fig. 5. Pressure was applied to the diaphragm at the backside of the sensor through the tubing which is tightly adhered to a holed plastic plate and the IOP sensor was stuck on top of this plastic plate. Nitrogen gas was used for the pressure measurement. The pressure of the nitrogen gas was detected real time by a Baratron pressure sensor (MKS Instruments, Andover, MA). A manually wound external power coil (5 turns, 3mm inner radius) was connected to the VNA and it was collinearly placed with the coil of the IOP sensor.

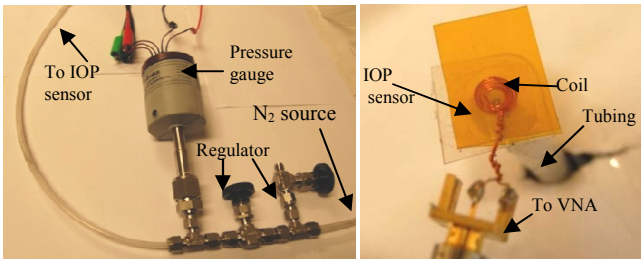

(a) (b)

Fig. 5. The pressure measurement setup: (a) gas control system; (b) IOP sensor and external coil

First, the impedance phase dip response of the external coil as a function of frequency was measured using the VNA under pressure range 0 - 60 mmHg at a distance of 2 mm away from the IOP sensor in air (Fig. 6). It shows very clear peak phase dip shift for different pressure levels. Measurements were repeated with varying distances between the external coil and the IOP sensor in the range of 2 - 7 mm both in air and saline solution.

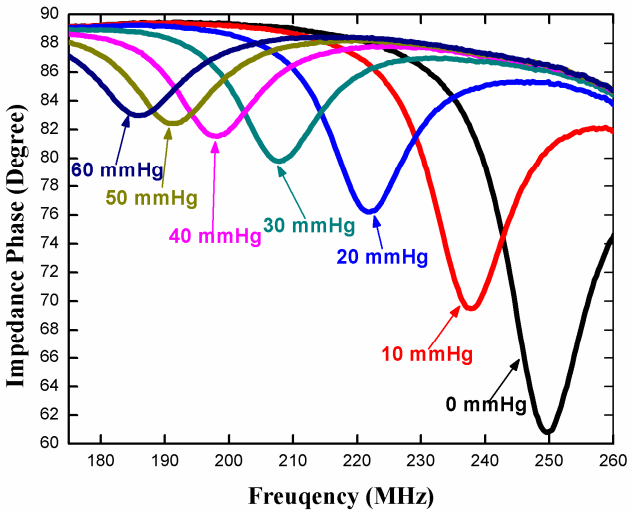

Fig.6. Peak phase dip frequency shift with varying pressures applied on the IOP sensor at 2 mm coils distance

Pressure sensitivity *S* can be defined as

$$S = \frac{\partial \frac{f_{min(P)}}{f_{min(P=0)}}}{\partial P}\Big|_{P=0}. \quad (6)$$

The peak phase dip frequency shift is proportional to square root of the capacitance change which can be described by

$$\frac{f_{min(P)}}{f_{min(P=0)}} = \sqrt{1 + \frac{\Delta C_s}{C_s}} \quad (7)$$

Assuming that deflection of the fully clamped diaphragm as a function of pressure (Fig. 2) is linear in the pressure range of interest (0 - 60 mmHg), peak phase dip frequency shift can be described by

$$\frac{f_{min(P)}}{f_{min(P=0)}} = \sqrt{1 + aP} \quad (8)$$

where a is empirical parameter that needs to be fit from the measurement data. Fig. 7 shows the normalized peak phase dip value of the IOP sensor as a function of pressure in air and in saline medium. The empirical parameter a can be obtained from curves of Fig. 7. Subsequently, based on the parameter a, sensitivities for both curves were obtained to be 7,050 ppm/mmHg in air and 3,770 ppm/mmHg in saline medium. It is clearly evident that the sensitivity in saline solution drops due to the high dielectric constant and conductivity property of saline solution. The responsivity of the SU-8-based IOP sensor was measured to be 1,083 KHz/mmHg in air and 683 KHz/mmHg in saline solution. Theoretically, this IOP sensor can have pressure resolution much lower than 1 mmHg both in air and in saline solution.

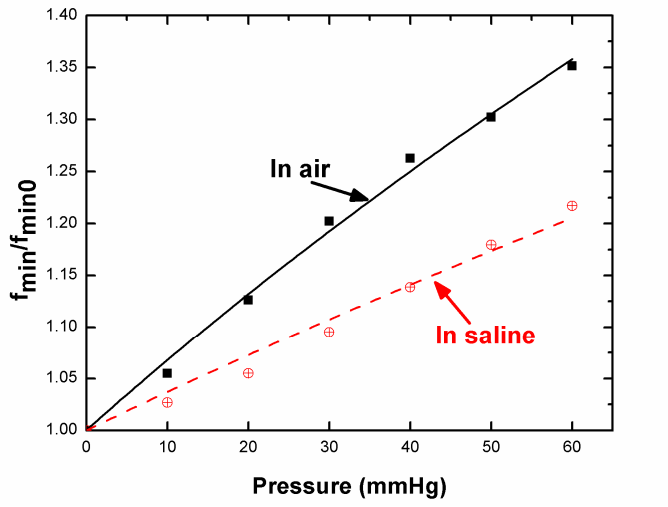

Fig. 7. Normalized peak phase dip frequency shift as a function of the applied pressure for the SU-8-based IOP sensor in the range of 0-60 mmHg in air and in saline solution

As expected, the peak phase dip in saline solution is smaller than that in air. With zero pressure, the peak phase dip in air was approximately 30 degree while it was approximately 5 degree in saline solution. However, the peak phase dip as a function of applied pressure is readily measurable in saline solution when the IOP sensor is placed within 6 mm distance from the external coil. Fig. 8 shows the magnitude of the peak phase dip as a function of distance between the external coil and the IOP sensor in saline solution with zero pressure. Beyond 4 mm distance, the phase dip drops dramatically and reaches nearly 0.3 degree at 6 mm, which is the maximum working distance. The working distance can be further increased by optimal design of the external coil.

V. CONCLUSION

A compact implantable SU-8-based passive wireless pressure sensor was designed, fabricated and characterized for intraocular pressure sensing application. It was found that the phase dip resonant frequency response is roughly proportional to the square root of pressure at the pressure range of interest (0 – 60 mmHg). By optimizing the thickness of the pressure sensitive membrane, fairly high sensitivity of 7,050 ppm/mmHg and responsivity of 1,083 KHz/mmHg of the IOP sensor in air were obtained. Future work will involve *in-vivo* pressure testing of the IOP sensor on the eye of animal to fulfill the continuous pressure monitoring.

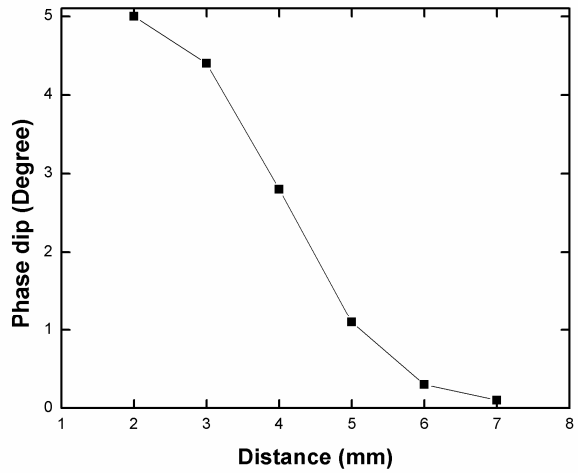

Fig. 8. Phase dip response as a function of the distance between external coil and the IOP sensor

ACKNOWLEDGMENT

The authors would like to acknowledge UT Dallas Cleanroom staffs for their support in this work.

REFERENCES

[1] S.-H. Cho, H. Lu, L. Cauller, M. Romero-Ortega and J.-B. Lee, "Biocompatible SU-8-based microprobes for recording neural spike signals from regenerated peripheral nerve fibers", *IEEE Sensors Journal*, vol. 8, no. 11, pp. 1830-1836, Nov. 2008.

[2] C. C. Collins, "Miniature passive pressure transensor for implanting in the eye," *IEEE Trans. Biomed. Eng.*, vol. BME-14, no. 2, pp. 74–83,
Apr. 1967.

[3] L. Rosengren, Y. Backlund, T. Sjostromt, B. Hok and B.Svedbergh, "A system for wireless intra-ocular pressure measurements using a slicon micromachined sensor,"*J. Micromech. Microeng.*, vol. 2, no. 3, pp. 202–204, Sept.1992.

[4] K.Van Schuylenbergh and R. Puers, "Passive telemetry by harmonics detection," presented at the 1996 Int. Conf. Medicine and Biological Engineering, Amsterdam.

[5] R. Puers, G. Vandevoorde, and D. D. Bruyker, "Electrodeposited copper inductors for intraocular pressure telemetry," *J. Micromech. Microeng.*,vol. 10, no. 2, pp. 124–129, Jun. 2000.

[6] P.-J. Chen, S. Saati, R. Varma, M. S. Humayun, and Y.-C. Tai, "Implantable flexible-coiled wireless intraocular pressure sensor," *J. Microelectromech. Syst.*, vol. 17, no. 6, pp. 1342–1351, Dec. 2008.

[7] G. Voskerician, M. Shive, R. Shawgo, H. V. Recum, J. Anderson, M.Cima, and R. Langer, "Biocompatibility and biofouling of MEMS drug delivery devices," *Biomaterials*, vol. 24, pp. 1959–1967, May. 2003.

[8] H. A. Wheeler, "Simple inductance formulas for radio coils," *Proc. IRE,* vol. 16, no. 10, pp. 1398-1400, Oct. 1928.